SLAC – PUB – 4532
January 1988
(T/AS)

LIMITS ON LATE DECAYING PARTICLES FROM NUCLEOSYNTHESIS*

SAVAS DIMOPOULOS
Department of Physics,
Stanford University, Stanford, California 94309

RAHIM ESMAILZADEH
Stanford Linear Accelerator Center,
Stanford University, Stanford, California 94309

LAWRENCE J. HALL
Department of Physics,
University of California, Berkeley, California 94720

GLENN D. STARKMAN
Department of Physics,
Stanford University, Stanford, California 94309

ABSTRACT

Late decaying ($\tau > 10^4$ sec) particles can alter the standard big bang predictions for the light element abundances. If $M > 10$ GeV, light element production and ^{4}He destruction can take place when hadronic decay products interact with the ambient protons and ^{4}He causing hadronic showers; depletion is the result of photodissociation by energetic decay photons. Previous works [1-4] putting limits on the properties of these particles ignored hadronic showers entirely, and usually considered only selected photodissociation reactions. We consider the full set of reactions and present both analytic and numerical bounds on the properties of particles with lifetimes greater than 10^4 sec. This drastically alters the limits on particle masses, lifetimes and abundances. For a gravitino lighter than a TeV, the reheat temperature must be less than 10^{10} GeV.

Submitted to *Nuclear Physics B*

* Work supported by the Department of Energy, contract DE-AC03-76SF00515.

1. Introduction

There has long been widespread interest in the possible existence of weakly interacting massive particles. Such particles, either stable or long-lived, arise naturally in many of the common extensions of the Standard Model, due to the inevitable presence of large mass scales and/or small effective low energy couplings to ordinary matter. They have been ascribed many magical properties and, in one form or another, can be shown to cure everything but the common cold. The great difficulty, however, lies in their detection since, of necessity, they have been kept well hidden from the prying eyes of low energy experiments.

One experiment which can hope to place limits on the properties of long-lived massive particles is the early universe. The observed entropy per baryon, the isotropy and spectrum of the background radiation, the abundances of the light elements, etc. all place limits on the masses, lifetimes and abundances of these exotics.

In two previous papers [5,6] (hereafter DEHS) we explored the effects of late-decaying ($\tau > 10^4$ sec), massive ($M > 10$ GeV) particles on big bang nucleosynthesis. We showed that, for a wide range of particle parameters, a late decaying particle could reproduce the observed light element abundances, independent of the results of any previous era of nucleosynthesis. This was true so long as at least the observed abundance of ^{4}He was produced in an earlier phase. In particular, we showed that this eliminates the bound on $\Omega_B h_o^2$ from Standard Big Bang Nucleosynthesis (SBBN), $0.03 > \Omega_B h_o^2$, and allows for a universe which is closed by baryons.

In this paper, we apply the techniques developed in the previous works to find the limits imposed by nucleosynthesis on the properties of unstable particles with lifetimes greater than 10^4 sec. The reader may at this point remark that the effects of late decaying particles have already been widely studied, with much work appearing in the literature. As discussed in some detail in DEHS, however, all previous work has invariably considered some subset of the operative reac-

tions and neglected all others, always without justification. For example, Ellis, Nanopoulos and Sarkar [1] set bounds on radiative decays of X's using the overproduction of D coming from ^{4}He photodissociation; however, they neglected the photodissociation of D, even though it has a much lower threshold. Others set bounds on the energy density in such particles by considering the photodissociation of deuterium by decay photons, ignoring the fact that deuterium is produced in the photodissociation of both ^{3}He and ^{4}He. One author [2] mistakenly neglected the photodissociation of heavier elements, arguing that since they are much less abundant a photon is unlikely to hit them; actually, the fractional decrease in an element's abundance due to photodissociation is independent of the abundance itself. Kawasaki and Sato [4] also ignored the photodissociation of ^{7}Li; in addition they started with a particular set of initial (SBBN) abundances and so got a stronger bound than if they had considered all possible initial conditions. Another author [3] included the effects of anti-nucleons, but entirely ignored nucleons. Energetic nucleons traveling through a KeV plasma undergo many strong interaction scatterings while thermalizing, thus producing baryonic showers. The entire phenomenon of baryonic showers and their effects on nucleosynthesis is discussed only in DEHS; it turns out to be *the dominant mechanism* for both the production of light elements and the destruction of ^{4}He as a result of massive particle decay. Our approach differs from our predecessors in that we write down all possible reactions, erase only those which do not affect the time evolution of the element abundances, and then proceed to solve the full set of equations — analytically where possible, numerically where not.

In chap. 2, we review the SBBN and DEHS models, as well as the relevant observations, and outline our philosophy and methodology for attacking this problem. In chap. 3, we study the equations for the light element abundances and use simple analytic arguments to constrain the allowed values of the mass, abundance, lifetime and hadronic branching ratio of the late decaying particle.

In chap. 4, we use the numerical solution of the equations for the light element abundances to further constrain these parameters. Finally, in chap. 5 we discuss our results and draw our conclusions.

2. Preliminaries

2.1 Standard Big Bang Nucleosynthesis

In 1967, Wagoner, Fowler and Hoyle [7] first calculated the abundances of the light elements formed in the early universe. The theory of Standard Big Bang Nucleosynthesis (SBBN) predicts the primordial abundances of hydrogen, deuterium, ^{3}He, ^{4}He, ^{6}Li and ^{7}Li as well as some higher mass elements as functions of η, the ratio of baryon to photon number densities, N_ν, the number of light neutrino species, and τ_n, the neutron lifetime (fig. 1). The philosophy of SBBN is to compare these predictions to observations and so constrain η and N_ν. Through this approach, one finds [8] that $N_\nu \leq 3$, and $3 \times 10^{-10} \lesssim \eta \lesssim 10^{-9}$. Since Ω_B, the ratio of the energy density in baryons to the critical density for closure, is proportional to η, this means $0.014 \leq \Omega_B h_o^2 \leq 0.03$.

2.2 Observations of the Light Elements

There are many fine reviews on observations of the light element abundances and the relationship between the primordial abundances and the observed abundances [9,10]. Here we present only the conclusions as they apply to this paper. Since our objective is to put reliable limits on properties of decaying particles, we work with the widest reasonable range of observed and inferred abundances.

Deuterium is detected mostly through the isotopic shift of lines of atomic H I and deuterated molecules, in stellar and planetary atmospheres and in the interstellar medium. Stellar D has not been detected; a conservative limit is $D/H < 10^{-6}$ 10. Boesgaard and Steigman take the most probable interstellar D/H value to be $0.8 - 2.0 \times 10^{-5}$, although Vidal–Madjar et al. [11] claim that $5 \times 10^{-6} - 5 \times 10^{-5}$ is consistent with observations. Observations of the Jovian troposphere [12] yield a D/H range of $1.2 - 3.1 \times 10^{-5}$.

To determine the primordial abundance of deuterium requires both an accurate determination of the current abundance and a complete theoretical un-

standing of its evolution. Deuterium has probably not been produced in significant quantities at any time in the history of the galaxy (see, however, Bond, Carr and Arnett [13]). Since any D which is processed through stars is completely destroyed, however, significant depletion may have occurred. The present abundance of D could be $1/2- < 1/20$ of its primordial value (for example, Pagel [14]). Therefore, all we can say reliably is that the primordial deuterium abundance was at least the present ISM abundance. We adopt as our lower bound for the ISM deuterium abundance 5.0×10^{-6} (unless otherwise specified, abundances are given as number densities compared to the number density of hydrogen).

Since ^{3}He can be both destroyed and produced in stars, its value as a probe of primordial nucleosynthesis is unclear. Arguments have been made [9] that observations of $D + {}^3$He are valuable. Theoretical models indicate that deuterium is completely processed into ^{3}He, while stellar ^{3}He destruction is only 25 to 50% efficient. Therefore, the observed stellar $D + {}^3$He can be used to place an upper bound on the primordial $D + {}^3$He. Presolar ^{3}He abundances inferred from meteorites and the solar wind are approximately $1 - 2 \times 10^{-5}$10. Measurements of ^{3}He in H II regions vary widely, with values as high as 1.5×10^{-4} [15,16]. We adopt as a tentative upper bound for the primordial ($D+ {}^3$He) 6×10^{-4}.

The best value for the primordial ^{4}He mass fraction Y_p comes from isolated extragalactic H II regions. Combined results from various authors give $Y_p = 0.245 \pm 0.003$ [17]). More recently, Steigman, Gallagher and Schramm [18] reported 0.235 ± 0.012. We take as our allowed range for Y_p 0.22 to 0.25.

There is an ongoing controversy whether the ^{7}Li abundance seen in low metallicity, halo dwarf stars ($\sim 5 \times 10^{-11}$ to $\sim 5 \times 10^{-10}$) reflects the true primordial abundance (e.g., Spite and Spite [19]), or whether the true primordial abundance is closer to that seen in Pop I stars ($\lesssim 2 \times 10^{-9}$). In DEHS we argued that the Pop II abundance was more likely to be primordial; however, since our objective here is to impose reliable bounds on particle physics, we do not wish to take

sides on this issue. We therefore consider a maximum range for the primordial ^{7}Li abundance to be 5×10^{-11} to 2×10^{-9}.

It is known from studies of the spectral lineshape that the lithium seen in the Pop II dwarfs is predominantly ^{7}Li and not ^{6}Li [20], although this may not reflect the primordial ^{6}Li/^{7}Li abundance ratio [5]. We will discuss the possible importance of ^{6}Li observations further in chap. 5.

2.3 DEHS-TYPE NUCLEOSYNTHESIS

In a previous paper [5], we investigated the effects of a late decaying ($\tau > 10^4$ sec) massive ($M \gtrsim 10$ GeV) particle, X, on the primordial abundances of D, ^{3}He, ^{4}He, ^{6}Li and ^{7}Li. Such a particle would decay after the era of standard nucleosynthesis, when the temperature of the universe has fallen to a few KeV. When a particle of mass greater than a few GeV decays during the KeV era, some of the energy goes into elecromagnetic decay products, and some goes into hadrons. Both classes of decay products form showers as they thermalize with the background plasma.

The baryonic decay products of X interact with the ambient protons and alpha particles and cause nuclear chain reactions that lead to the production of the light nuclei D, ^{3}He, ^{6}Li, ^{7}Li and destruction of ^{4}He. In DEHS, we calculated ξ_n, ξ_d,$\xi_{^3\mathrm{H}}$, $\xi_{^3\mathrm{He}}$,$\xi_{^6\mathrm{Li}}$ and $\xi_{^7\mathrm{Li}}$, respectively the average number of low energy neutrons, deuterons, tritons, ^{3}He, ^{6}Li and ^{7}Li nuclei, produced per X decay; $\xi_{^4\mathrm{He}}$, the average number of alpha particles scattered out of the thermal sea to MeV energies; and ξ_α^K, the number of alpha particles destroyed. The results are listed in Table 1. In calculating the ξ_i, we took the baryon multiplicity and the primary baryon energy for $M_X = 1$ TeV; $\nu_B = 5$ and $E_{in} = 5$ GeV. The number and energy of the primary baryons actually depends weakly on the mass of the X. The value of ν_B, however, can be absorbed into an effective baryonic branching ratio,

$$r_B^* = r_B \frac{\nu_B}{5} \mathcal{F} \quad . \tag{2.1}$$

Here r_B is the true baryonic branching ratio, and $\mathcal{F}$ is a factor which represents the dependence of the yields, ξ's, on the energy of the primary shower baryons. For a more detailed discussion, see DEHS.

When a massive X decays electromagnetically or hadronically, it injects very energetic photons, electrons and positrons into the relatively cool (T = 1–30 KeV) background plasma. The development of the ensuing shower had been studied previously [21] and is described in detail in DEHS. The photons are found to have a spectrum

$$\xi_\gamma(E) = \begin{cases} \frac{M_X}{2E_{max}^{1/2}} E^{-3/2} & 0 \leq E \leq E_{max} \\ 0 & E_{max} \leq E \ , \end{cases} \tag{2.2}$$

with $E_{max} \sim m_e^2/25T$ due to the overwhelming effectiveness of electron-positron pair production of thermal photons. As the temperature falls, E_{max} rises above the photodissociation thresholds of the various light elements and they become vulnerable to photodestruction.

The existence of both baryonic and electromagnetic showers means that DEHS-type nucleosynthesis has means of both producing and destroying all the light elements (except ^{4}He which is destroyed by both types of showers). The relative values of $f_X^0 r_B^*/f_B$, which governs production, and $f_X^0 M_X/f_B$ and τ, which govern destruction, as well as possibly the element abundances at the onset of DEHS, govern the final element abundances. For a more in-depth treatment, see DEHS.

2.4 Entropy Production and the Time-Temperature Relation

When X's decay, they increase the entropy per moving volume of the universe; this alters the connection between the scale factor, R, and the temperature, T, and hence modifies the time-temperature relation. Scherrer and Turner [22] showed that when the entropy of the universe is dominated by relativistic particles, and the entropy released by the decaying X particles is thermalized on

time scales short compared to the Hubble time, then the equations governing the evolution of the scale factor, the temperature and the entropy, S, in a co-moving volume R^3, are:

$$\rho_x = \rho_{x_o}(R_o/R)^3 \exp(-t/\tau) \tag{2.3}$$

$$\dot{S} = R^3 \rho_x / T\tau \tag{2.4}$$

$$(\dot{R}/R)^2 = \frac{8\pi G}{3}(\rho_r + \rho_m + \rho_o) \tag{2.5}$$

$$\rho_r = \left(\frac{3}{4}\right)\frac{2\pi^2 g_\star}{45} T^4 \tag{2.6}$$

$$S = \frac{2\pi^2 g_\star}{45}(RT)^3 \tag{2.7}$$

where ρ_i is the energy density in species i, and $g_\star$ is the number of effective relativistic degrees of freedom. These equations can be integrated numerically to obtain R, S, and T as a function of time.

2.5 Equations Governing the Light Element Abundances

Equipped with the ξ's and with a time-temperature relation, we can write down the equations governing the abundances of the light elements during the period of X decay.

We define $f_i(t)$ to be the reduced number density of species i, the number density at time t of species i, divided by the number density $n^o_{\gamma_{th}}$ of thermal photons at time $t_o \approx 10^2$ sec diluted by $(R_o/R)^3$, the expansion of a comoving volume since the time t_o. Note that this differs slightly from the definition of DEHS, since in that work entropy dilution could be neglected; this is not the case for the larger region of parameter space included in this work. Also, in DEHS we were interested in a region of parameter space for which the final light element abundances are independent of the abundances produced by SBBN (except of course for ^{4}He). Therefore, we were not concerned with getting those SBBN

predictions exactly right. In this work the transition from SBBN to DEHS is crucial, hence we include in our analysis not only the reactions detailed in DEHS 1987a, but also the SBBN reactions included in the Wagoner code as updated by Kowano [8]. It emerges that for the shortest lifetimes considered ($\tau = 10^4$ sec), DEHS processes begin to affect the element abundances after $t \approx 200$s while SBBN processes have been effectively shut off by $t \approx 10^4$ sec.*

For purposes of the numerical work outlined in chap. 5, we use the full set of equations described above; for the analytic bounds derived in chap. 4, we confine ourselves to the equations given in DEHS, using the final SBBN values as input. Since DEHS and SBBN do not actually occur in complete isolation of each other, the validity of the analytic treatment can only really be demonstrated *a posteriori*. To understand the uncertainties in both the analytic and the numerical calculations, we refer the reader to sec. 4.5 of DEHS. It is important to note that the dependence of the equations on the particle physics is entirely contained in the four particle parameters: $f_x M_x$, which determines the photodissociation strength, $f_x r_B^*$, which determines the amount of hadro-production/destruction, τ_x and η, which determines the element abundances in the SBBN framework (for a fixed N_ν and τ_n).

2.6 Assumptions and Methodology

Before we discuss how we place both analytic and numerical limits on particle parameters, we summarize our assumptions:

1) We assume that SBBN accurately predicts the light element abundances at $\sim 2 \times 10^2$ sec. This constrains us in two ways. First, we must take $\tau \gtrsim 10^4$ sec, so that the X decay products at 200 sec are unimportant. For $\tau < 10^4$ sec, if the energy density in X particles were low enough, there would also be no effect; however, such an X would clearly be impotent after SBBN.

* The fact that both DEHS and SBBN processes are important between ~ 200 sec and $\sim 10^4$ sec, has a slight effect on the ^{4}He production. This requires a small [O(50%)] change in the value of $f_X^o r_B^*/f_B$ quoted in DEHS.

2) Second, we take $f_X^o M_X / f_B < 6 \times 10^4 \times 2.8 \times 10^{-8}/\eta$, so that the X energy density is low enough not to significantly affect the time temperature relation during SBBN (Turner and Scherrer). We also neglect the effects of other exotic physics, such as the quark-hadron phase transition.

3) For our analytic bounds we actually assume that SBBN is completed before the onset of DEHS, and use the final SBBN abundances. This is certainly true at the 50% level at worst, but this is not easily justified except by comparison with numerical results.

4) We treat only particles with lifetimes $\tau \leq 10^7$ sec. This upper bound comes from limits on the spectrum of the microwave background radiation. Clearly, if the energy density in X's is very small compared to the energy density of the radiation, this bound can be evaded.

5) We assume that there is only one type of X particle.

6) We assume that this particle is uncharged, colorless and carries no baryon number, and that its decays are not baryon-number violating.

7) We assume that the fraction of the particle mass which does not end up as photons is negligible. For any particle for which this is not the case, one can replace the mass in any bound by the average energy per decay which does go into photons. This is true so long as X and its nonrelativistic decay products do not dominate the energy density of the universe before essentially all the X's have decayed.

8) We assume that the time scale for thermalization is much less than the Hubble time at all times of interest.

Given these assumptions we adopt the following methodology. For each set of particle parameters, $f_x M_x$, $f_x r_B^*$ and τ_x , we seek an η such that the final light element abundances do not conflict with observations. By this we mean that the ^{4}He mass fraction is between 0.22 and 0.25, that ^{7}Li H lies in the range 5×10^{-11} to 2×10^{-9}, and that $D/H > 5 \times 10^{-6}$. (As discussed above, we regard the D +

^{3}He and ^{6}Li bounds as less reliable and consider them separately.) If we find such an η, then the particle parameters are not forbidden by nucleosynthesis.

In chap. 4, we attempt to constrain our parameter space analytically as much as possible before embarking on a numerical survey in chap. 5. This is crucial for reducing the parameter space, so that the numerical work can be performed using a finite amount of computing time. More importantly, the analytic bounds are interesting on their own, since they are simple and can easily accommodate improvements in the astronomical observations and the nuclear experimental data.

3. Analytic Bounds

As discussed in chap. 2, for each set of particle parameters, $f_X^o M_X/f_B$, $f_X^o r_B^*/f_B$ and τ_X, we seek an η such that the final element abundances do not conflict with observations. With this in mind, we start in sec. 3.1 by identifying an allowed region of (low) $f_X^o M_X/f_B$ and $f_X^o r_B^*/f_B$, in which the effects of the X are negligible and the abundances of SBBN are not disturbed sufficiently to conflict with observations. In secs. 3.2 and 3.3, we consider the evolution of the ^{4}He and ^{7}Li abundances, respectively. For each η, this enable us to identify, analytically, regions in which excessive destruction or production of these elements occurs, and which can therefore be excluded. In sec. 3.3 we also show how these η-dependent bounds can be combined to give η-independent bounds, allowing us to identify regions which can be excluded for all η. In sec. 3.4, we identify the problems with bound coming from deuterium. Finally, in sec. 3.5 we summarize and discuss the analytic limits on the particle parameters.

We first recall those abundance equations which will be necessary to obtain these analytic bounds.

The equations governing the light element abundances are approximately:

$$\dot{f}_{\gamma^*}(E) = \xi_{\gamma^*}(E) f_X^o \Gamma_X e^{-t/\tau_X} - f_{\gamma^*}(E) f_e n_{\gamma_{th}} c\sigma_C(E) \tag{3.1}$$

$$\dot{f}_d = r_B^* \xi_d f_X^o \Gamma_X e^{-t/\tau_X} - f_d {n_{\gamma_{th}}}^o \int_0^{E_{max}} f_{\gamma^*}(E) c\sigma_{d\gamma}^D(E) dE \tag{3.2}$$

$$\dot{f}_\alpha = -r_B^* \xi_\alpha^K f_X^o \Gamma_X e^{-t/\tau_X} - f_\alpha {n_{\gamma_{th}}}^o c \int_0^{E_{max}} f_{\gamma^*}(E) \sigma_{\gamma\alpha}^D(E) dE \tag{3.3}$$

$$\dot{f}_7 = r_B^* \xi_7 f_X^o \Gamma_X e^{-t/\tau_X} - f_{^7\mathrm{Li}} {n_{\gamma_{th}}}^o \int_0^{E_{max}} f_{\gamma^*}(E) c\sigma_\gamma^{D\,^7\mathrm{Li}}(E) dE \tag{3.4}$$

where we have neglected neutron capture processes for d and ^{7}Li as well as d production by ^{3}He, ^{3}H and α photodissociation, all of which can be ignored for the purposes of the analytic estimates. Here σ_C is the Compton cross section, σ^D 's are photodissociation cross sections, and f_X^o is the number density of X's divided by the number density of thermal photons, after the X's fall out of thermal equilibrium. In the photon equation, $f_{\gamma^*}(E)$ represents the reduced number density of photons with energy between E and E + dE, and A and A' represent any light nuclei.

3.1 ALLOWED REGION

The predictions of SBBN agree with observations for a range of η, $3\times10^{-10} \lesssim \eta \lesssim 10^{-9}$. If $f_X^o r_B^*/f_B$ is small, then DEHS nucleosynthesis cannot induce significant hadroproduction or hadrodestruction of the light elements. Similarly, if $f_X^o M_X/f_B$ is small, then photodissociation is suppressed. We now determine how small $f_X^o r_B^*$ and $f_X^o M_X/f_B$ have to be not to affect the light element abundances.

We first consider the effects of hadroproduction only. The change in the reduced number density of element i due to hadroproduction is $\xi_i f_X^o r_B^*$. If $f_i^{all,min}$ is the minimum amount of species i produced during SBBN, for the SBBN allowed range of η, and $f_i^{ob,max}$ is the maximum amount of species i allowed within the observational limits, then we must have:

$$\frac{f_X^o r_B^*}{f_B} < \frac{f_i^{ob,max} - f_i^{all,min}}{f_B} \frac{1}{\xi^{i,max}} \quad i = 2,7 \tag{3.5}$$

where ξ_i^{max} is the maximum value of ξ_i within the uncertainties computed in DEHS; and

$$\frac{f_X^o r_B^*}{f_B} < \frac{f_4^{all,max} - f_4^{ob,min}}{f_B} \frac{1}{|\xi_\alpha^K|^{max}} \quad i = 2,7 \quad . \tag{3.6}$$

The strongest bound comes from ^{7}Li, with $f_7^{ob,max} = 2 \times 10^{-10} f_B$, $f_7^{all,min} = 5 \times 10^{-11} f_B$, and $\xi_7 \leq 1 \times 10^{-5}$. This gives $f_X^o r_B^*/f_B < 1.5 \times 10^{-5}$ for the allowed values of $f_X^o r_B^*/f_B$.

Note that we have used $f_7^{ob,max} = 2 \times 10^{-10} f_B$, not $2 \times 10^{-9} f_B$. This is so as not to claim as definitely allowed, values of $f_X^o r_B^*/f_B$ which lead to ^{7}Li abundances inconsistent with the Pop II abundances being primordial (DEHS 1987a). A similar upper limit on the allowed region is also obtained by requiring the quite strict $D + {}^3\mathrm{He} < 10^{-4}$. Much stricter upper limits ($f_X^o r_B^*/f_B < 3 \times 10^{-7}$) are obtained if one believes that the upper limit on ^{6}Li from Pop II dwarfs, $f_6^{ob,max} < 10^{-11} f_B$, reflects primordial abundances.

We now consider the effects of photodissociation. The allowed values of $f_X^o M_X/f_B$ are determined by the condition that photodissociation of all the light elements be insignificant. Considering photodissociation alone, the equations for the light elements can be integrated to obtain

$$f_i(t=\infty) = \exp\left(-\int_{t_i}^{\infty} \Gamma_i dt\right) f_i(t_i) \quad , \tag{3.7}$$

where

$$\begin{aligned} \Gamma_i(t) &= \int_{Q_i}^{E_{max}} n^o_{\gamma_{th}} f_{\gamma^*}(E) \sigma_i^D(E) dE \\ &= \left(\frac{f_X M_X}{f_B \text{ GeV}}\right) 10^3 \frac{f_B}{f_e} \left(\frac{\sigma^C(1 \text{ MeV})}{mb}\right)^{-1} e^{-t_i/\tau} \mathcal{F}_i \quad . \end{aligned} \tag{3.8}$$

$\mathcal{F}_i$ is the dimensionless integral

$$\mathcal{F}_i = e^{t_i/\tau} \int_{t_i}^{\infty} e^{-t/\tau} \frac{dt}{\tau} \int_{Q_i}^{E_{max}(t)} \frac{E^{-1/2}}{2\sqrt{E_{max}}} \frac{\sigma_i^D(E)}{mb} dE, \tag{3.9}$$

where Q_i is the photodissociation threshold of species i, and t_i is the time at which i becomes vulnerable to photodissociation. For D, ^{3}He and ^{7}Li, this means that

$$\exp\left(-\int_{t_i}^{\infty}\Gamma_i dt\right) f_i^{all,max} > f_i^{ob,min} \quad . \tag{3.10}$$

For ^{4}He we must impose the stricter condition that no significant D or ^{3}He production occur. The question of what is "significant" is subtle, but largely unimportant. We take it conservatively to be the observational minimum deuterium abundance; thus,

$$\left[1-\exp\left(-\int_{t_4}^{\infty}\Gamma_4 dt\right)\right] f_4^{all,max} \lesssim f_2^{ob,min} \quad . \tag{3.11}$$

For $\tau \ll t_4$, ^{4}He photodissociation is strongly suppressed and the strictest bound comes from deuterium and ^{7}Li; for $\tau \gtrsim t_4$, ^{4}He is more constraining. To obtain a tau independent bound, we take the strictest bound, which is obtained by using the maximum allowed tau.

3.2 ^{4}He Destruction

The simplest limit is obtained by forbidding excessive hadrodestruction of ^{4}He. Therefore, the region defined by

$$\frac{f_X^o r_B^*}{f_B} > \frac{f_4^{p,max} - f_4^{ob,min}}{f_B}\frac{1}{|\xi_\alpha^K|^{min}} \quad i=2,7 \tag{3.12}$$

is forbidden. Here $f_4^{p,max}$ is the maximum ^{4}He produced in the range of η under consideration. We took $f_4^{p,max} = 7.510^{-2} f_B$ and $f_4^{ob,min} = 5.510^{-2} f_B$, corresponding to Y=0.30 and Y=0.22, respectively.

As discussed above, integrating the ^{4}He equation in the absence of hadrodestruction, one obtains

$$f_4(t=\infty) = \exp\left(-\int_{t_4}^{\infty} \Gamma_4 dt\right) f_4(t_4) \quad . \tag{3.13}$$

Therefore, the region defined by

$$\frac{f_X M_X}{f_B \text{ GeV}} > 10^{-3} \quad \frac{\sigma^C(1 \text{ MeV})}{mb} \frac{f_e}{f_B} \frac{1}{\mathcal{F}_4} \quad e^{t_4/\tau} \quad \ln\left(\frac{f_4^{p,max}}{f_4^{ob,min}}\right) \tag{3.14}$$

is forbidden, due to excessive photodissociation of ^{4}He. In fig. 2, we graph $\mathcal{F}_4 \exp(-t_4/\tau)$ versus τ, it is approximately independent of $f_X^o M_X/f_B$.

One can also derive more general η-dependent bounds, combining hadrodestruction and photodissociation of ^{4}He. Without solving the full rate equation, one can see that the final ^{4}He abundance must fall between

$$\frac{f_4^{min}}{f_B}(\eta) = \exp\left\{-\frac{f_X M_X}{f_B \text{ GeV}} e^{-t_4/\tau} \mathcal{F}_4 10^3 \frac{mb}{\sigma^C(1 \text{ MeV})} \frac{f_B}{f_e}\right\} \frac{f_4^p}{f_B}(\eta) - \frac{f_X^o r_B^* |\xi_\alpha^K|^{max}}{f_B} \tag{3.15}$$

and

$$\frac{f_4^{max}}{f_B}(\eta) = \exp\left\{-\frac{f_X M_X}{f_B \text{ GeV}} e^{-t_4/\tau} \mathcal{F}_4 10^3 \frac{mb}{\sigma^C(1 \text{ MeV})} \frac{f_B}{f_e}\right\} \left(\frac{f_4^p}{f_B}(\eta) - \frac{f_X^o r_B^* |\xi_\alpha^K|^{min}}{f_B}\right) \quad . \tag{3.16}$$

The minimum abundance is obtained by allowing photodissociation to act on the initial abundance ignoring hadrodestruction, and then doing all the hadrodestruction at the end. The maximum abundance is obtained by doing all the hadrodestruction initially and then photodissociating. Limits are obtained by demanding that f_4^{min} be greater than $f_4^{ob,min}$ and f_4^{max} be less than $f_4^{ob,max}$. The η independent bounds on $f_X^o M_X/f_B$ and $f_X^o r_B^*/f_B$ quoted above can be obtained by ignoring photodissociation and hadrodestruction, respectively, and taking the weakest limit for all η.

3.3 ^{7}Li Destruction and Production

As for ^{4}He, we obtain η dependent bounds on $f_X^o M_X/f_B$ and $f_X^o r_B^*/f_B$ by requiring that f_7^{max} be greater than $f_7^{ob,min}$ and f_7^{min} be less than $f_7^{ob,max}$, where now

$$\frac{f_7^{max}}{f_B}(\eta) = \exp\left\{-\frac{f_X M_X}{f_B \text{ GeV}} e^{-t_7/\tau} \mathcal{F}_7 10^3 \frac{mb}{\sigma^C(1 \text{ MeV})} \frac{f_B}{f_e}\right\} \frac{f_7^p}{f_B}(\eta) + \frac{f_X^o r_B^* \xi_7^{max}}{f_B} \tag{3.17}$$

and

$$\frac{f_7^{min}}{f_B}(\eta) = \exp\left\{-\frac{f_X M_X}{f_B \text{ GeV}} e^{-t_7/\tau} \mathcal{F}_7 10^3 \frac{mb}{\sigma^C(1 \text{ MeV})} \frac{f_B}{f_e}\right\} \left(\frac{f_7^p}{f_B}(\eta) + \frac{f_X^o r_B^* \xi_7^{min}}{f_B}\right) \tag{3.18}$$

In fig. 3, we plot $\mathcal{F}_7 \exp(-t_7/\tau)$ as function of τ; it is also essentially independent of $f_X^o M_X/f_B$ for the range of $f_X^o M_X/f_B$ of interest. η independent bounds can be obtained by enforcing the weaker conditions

$$f_7^{ob,max} > \min_{\eta} f_7^{min}(\eta) \tag{3.19}$$

$$f_7^{ob,min} < \max_{\eta} f_7^{max}(\eta) \quad . \tag{3.20}$$

The first bound requires that if one starts with the minimum ^{7}Li abundance possible from SBBN, and hadroproduces ^{7}Li to the extent that its abundance exceeds the observational maximum, then one must photodestroy some of that ^{7}Li, so that the final abundance agrees with observations. It can be easily shown that the destruction of ^{7}Li by neutron capture is negligible compared to its production in hadron showers, and can be ignored.

The second bound requires that if one starts with the maximum ^{7}Li abundance possible from SBBN, and photodestroys ^{7}Li to the extent that its abundance falls below the observational minimum, then one must hadroproduce some ^{7}Li, so that the final abundance agrees with observations.

Various limiting cases are of interest. The minimum value of $f_X^o M_X/f_B$ such that ^{7}Li production is required to compensate for photodissociation is

$$\left(\frac{f_X M_X}{f_B \text{ GeV}}\right)_{min} = 10^{-3} \ \frac{\sigma^C(1 \text{ MeV})}{mb} \frac{f_e}{f_B} \frac{1}{\mathcal{F}_7} \ e^{t_7/\tau} \ \ln\left(\frac{f_7^{p,max}}{f_7^{ob,min}}\right) \quad . \tag{3.21}$$

In the limit of large $f_X^o M_X/f_B$, we find that

$$\frac{f_X^o r_B^*}{f_B} \geq \frac{1}{\xi_7^{max}} \frac{f_7^{ob,min}}{f_B} \quad . \tag{3.22}$$

The minimum $f_X^o r_B^*/f_B$ such that ^{7}Li photodissociation is required to compensate for ^{7}Li overproduction is

$$\frac{f_X^o r_B^*}{f_B} = \frac{1}{\xi_7^{min}} \frac{f_7^{ob,max} - f_7^{p,min}}{f_B} \quad . \tag{3.23}$$

Note that in all the above limits, $f_X^o M_X/f_B$ appears only in the combination $f_X^o M_X/f_B \mathcal{F}_7 \exp(-t_7/\tau)$, so that only limits on this quantity can be obtained.

3.4 Deuterium Production/Destruction

Deuterium is less valuable than one might hope in setting analytic bounds on the particle parameters. As stated earlier, we intend to make use only of the lower limit on observed deuterium. Since, in the standard model of the chemical evolution of the galaxy, deuterium is not made in stars this is also a lower bound for the primordial deuterium abundance. One would hope that one could impose the condition that the minimum possible deuterium abundance be greater than the observed minimum. Unlike ^{7}Li, however, deuterium is not produced only in baryonic showers; it is also a byproduct of ^{4}He and ^{3}He photodissociation and of neutron capture by protons. Neutrons are made not only in baryonic showers, but also in the photodissociation of other light elements. All these complications make obtaining a useful bound very difficult. Moreover, when $D+$ ^{3}He is underproduced, ^{4}He tends to be overproduced, and the requirement to destroy some ^{4}He is usually stronger than any limits from deuterium.

3.5 Discussion of Analytic bounds

In fig. 4, we graph the η-independent bounds in the $f_X^o r_B^*/f_B$ versus $f_X^o M_X/f_B$ $\exp(-t_7/\tau)\mathcal{F}_7$ plane; together with the graphs of $\exp(-t_i/\tau)\mathcal{F}_i$, this allows one to determine whether a given set of values of $f_X^o M_X/f_B, f_X^o r_B^*/f_B$ and τ are forbidden or allowed by analytic arguments. Note that those points which fall in neither region can neither be allowed nor forbidden by simple analytic arguments; their status will be determined in chap. 4, where we solve the evolution equations numerically.

The configuration of the limits is easily understood:

a) In the lower left is region (a), where one neither produces nor destroys significant fractions of the SBBN abundances. Since SBBN agrees with the observations for a range of η, and since in this region the energy density in X's is far too low to affect the SSBN era nucleosynthesis directly, this region of parameter space is "super-allowed."

b) Above the allowed region is a forbidden zone, region (b). If one produces enough ^{7}Li to put even the lowest possible SBBN above the maximum observed value, then one must photodissociate some of it. The more one makes, the more one must photodissociate.

c) In region (c) one has allowed too much hadrodestruction of ^{4}He, bringing it down from the maximum that SBBN can produce, below the minimum consistent with observations.

d) If one starts with the maximum ^{7}Li abundance produced by SBBN, and photodissociates it to below the minimum observed primordial abundance, then one must begin producing it. The more one destroys, the more one must produce. Since, however, in determining the maximum abundance that one can end up with, one ignores the photodissociation of what is produced, therefore, even for very large values of $f_X^o M_X/f_B$, the minimum $f_X^o r_B^*/f_B$ is never more than what is required to produce the observed lower limit of ^{7}Li. This is region (d).

The region of excessive ^{4}He photodissociation is far to the right of the region seen in the figure, for $\tau < 10^7 \simeq t_7$.

It is reassuring that the region identified in DEHS is not within the forbidden zones.

4. Numerical Results

The SBBN and DEHS equations were integrated numerically on a combination of a Micro–VAX, an IBM–3081 and the SDSC CRAY. The SBBN code of Wagoner as modified by Kowano [8] was run up to $\sim$ 200 sec and used as input to the DEHS code [5] modified to include those SBBN reactions which are still active at 200 sec, as well as the time-temperature relation described in chap. 3. The choice of 200 sec was made because at this time DEHS effects are not yet important while most of the SBBN nucleosynthesis has ended. This eliminated the necessity of running the SBBN code up to 200 sec for different particle parameters.

The SBBN code was run for a selection of eleven η's between 9×10^{-11} and 3×10^{-8} which mapped out the full variation of the final SBBN values. The DEHS code was then run for τ's from $10^4 - 10^7$ sec for $f_X^o M_X/f_B$'s from $10^{-3} - 10^6$. Since for fixed η, τ and $f_X^o M_X/f_B$ the final ^{4}He abundance is linear in $f_X^o r_B^*/f_B$, the code was run for $f_X^o r_B^*/f_B$'s giving ^{4}He between 0.20 and 0.27. In total, the code was run for approximately 6,000 data points.

Once the results were obtained, the data was analyzed to see for what particle parameters an η could be found such that the final element abundances fell within the allowed region: $0.22 < Y < 0.25$, $5 \times 10^{-6} < D$, $8 \times 10^{-11} <^7 \mathrm{Li} < 2 \times 10^{-9}$ (here Y is the mass fraction of ^{4}He, all other abundances are number densities compared to hydrogen). The results are shown in fig. 5.

As expected, the points in the allowed region(s) fall into two broad classes. The easiest to understand are those points for which η falls into the range allowed by SBBN, and both $f_X^o M_X/f_B$ and $f_X^o r_B^*/f_B$ are too low to affect the abundances significantly. These are to be found in the large regions in the lower left of the graphs. The top boundary of this region is given by excessive ^{7}Li hadroproduction. The right-hand boundary is given by overdissociation of D, ^{4}He, or ^{7}Li depending on the particular value of τ.

The other points are, in general, of the type identified in refs. 5 and 6 for which the abundances have reached fixed point values (for a more detailed discussion, see DEHS). These are the points in the middle of the graphs. This region is most clearly identifiable for $\tau = 5 \times 10^4$ sec. Here the top boundary is again from excessive hadrodestruction of ^{4}He, and the right boundary from overdissociation of ^{7}Li. The bottom is from underproduction/overdissociation of deuterium, and the left boundary is from underdissociation of ^{7}Li. This description also holds for other τ's where these points are found, although the separation of the two regions is less clear.

It is instructive to note that, as the upper bound on the primordial $D + {}^3$He or ^{6}Li is decreased from our quoted values, the DEHS-type points are eliminated from the allowed region. This would restore the traditional bounds on η.

5. The Gravitino: Limits on the Reheat Temperature

Many of the previous efforts to put limits on late decaying massive particles from nucleosynthesis, were made in the context of the so-called "gravitino problem." Gravitinos are produced in the reheating phase of the inflationary universe. The number density after inflation of gravitinos with mass $M_{3/2}$ is given by

$$f_{3/2}(t) = 2.35 \times 10^{-13} \frac{T_R}{10^9 \text{ GeV}} \left(1 - 0.018 \ln \frac{T_R}{10^9 \text{ GeV}}\right) \quad . \tag{5.1}$$

This can be combined with our bound on f_X:

$$\frac{f_X M_X}{f_B \text{ GeV}} < \begin{cases} \mathcal{G}(\tau) & \text{SBBN} \\ \mathcal{H}(\tau) & \text{DEHS} \end{cases} \tag{5.2}$$

where $\mathcal{G}(\tau)$ and $\mathcal{H}(\tau)$ are graphed in fig. 6. We thus obtain the bound

$$T_R < 4 \times 10^{12} \text{GeV} \left(\frac{\Omega_B h_o^2}{3 \times 10^{-2}}\right) \left(\frac{\text{GeV}}{M_X}\right) \times \\ \times \left(\frac{1}{1 - 0.018 \ln \frac{T_R}{10^9 \text{ GeV}}}\right) \begin{cases} \mathcal{G}(\tau) & \text{SBBN} \\ \mathcal{H}(\tau) & \text{DEHS} \end{cases} \quad . \tag{5.3}$$

Using the mass lifetime relation

$$\tau = 4 \times 10^8 \text{ sec } \ (100 \text{ GeV/M})^3 \frac{1}{N_c} \tag{5.4}$$

(where N_c is the number of channels into which the gravitino can decay), we can find the limit on T_R as a function of $M_{3/2}$. We graph this over the range of applicable M's for a variety of N_c's for both the SBBN and DEHS scenarios in fig. 1. We can also obtain r_B^*-dependent bounds:

$$T_R^{SBBN} < \frac{4 \times 10^8 \text{ GeV}}{r_B^*} \left(\frac{\Omega_B h_o^2}{3 \times 10^{-2}}\right) \tag{5.5}$$

$$T_R^{DEHS} < 4 \times 10^{11} / r_B^* \quad . \tag{5.6}$$

These differ from previously obtained bounds because of the improved treatment of the physics of the decaying X. For example, the bounds of Ellis, Nanopoulos

and Sarkar [1], Dominguez–Tenreiro [2], Kawasaki and Sato [4], Linde [3] and all others are invalid because they left out the most important processes, as discussed in the introduction. We conclude that if the $\tilde{G}$ is lighter than a TeV, T_R must be less than 10^{10} GeV. This is a powerful constraint and requires either that baryogenesis occurs at a low temperature or that the above bound on T_R is invalidated by subsequent entropy dilution (i.e., very low temperature inflation).

6. Conclusion

We have presented the analytic and numerical bounds on the abundance, mass, lifetime and hadronic branching ratio of long lived (10^4 sec $< \tau < 10^7$ sec) particles. These are summarized in fig. 5. It emerges that, as long as the upper bounds on $D + {}^3\mathrm{He}$ and ${}^6\mathrm{Li}$ are not too low, there are allowed points for a wide range of values of η previously forbidden by SBBN. If the bounds on these primordial abundances are lowered, then only SBBN allowed η values remain.

The value of improved ${}^6\mathrm{Li}$ measurements both for testing the DEHS hyptothesis and for strengthening the bounds on particle properties is clear. This is due to the high yields of ${}^6\mathrm{Li}$ in baryonic showers, and is to be contrasted with the situation in SBBN where scant ${}^6\mathrm{Li}$ production occurs and ${}^6\mathrm{Li}$ has little value as a probe. Improved ${}^6\mathrm{Li}$ measurements are anticipated in the near future .

We also present updated limits on the reheating temperature in inflationary universes containing gravitinos with lifetimes in the range 10^4 s $< \tau < 10^7$ sec.

Acknowledgements

We would like to acknowledge Larry Kowano for the use of his modified Wagoner code, NUC123, as well as for instructions in its use. We would also like to thank Jeff Martoff for the use of his computer, the purchase of which was made possible by a grant from the Pew Memorial Trust to Stanford University. Numerical work reported this paper was also performed on the IBM 3081 at the Stanford Linear Accelerator Center, and on a CRAY at the San Diego Supercomputer Center, under a Stanford University seed grant. S. D. and G. D. S. acknowledge support by the National Science Foundation under Grant NSF–PHY–86–12280 to Stanford University. G. D. S. is a National Science and Engineering Research Council of Canada Postgraduate Scholar. R. E. acknowledges support by the Department of Energy, contract DE–AC03–76SF00515 at SLAC. L. J. H. acknowledges support by the Director, Office of Energy Resources, Office of High Energy and Nuclear Physics, Division of High Energy of the U. S. Dept. of Energy under contract DE–AC03–7600098 and in part by NSF under Grant PHY–85–15857. L. J. H. also acknowledges partial support by a Sloan Foundation Fellowship and a Presidential Young Investigator Award.

REFERENCES

1. J. Ellis, D. V. Nanopoulos and S. Sarkar, Nucl. Phys. **259** (1985) 175.
2. R. Dominguez–Tenreiro, Ap. J. **313** (1987) 523.
3. M. Yu. Khlopov and A. D. Linde, Phys. Lett. **138B** (1984) 265.
4. N. Kawasaki and K. Sato, Phys. Lett. **189B** (1987) 23.
5. S. Dimopoulos, R. Esmailzadeh, L. Hall and G. Starkman, Phys. Rev. Lett. **60** (1988) 7.
6. S. Dimopoulos, R. Esmailzadeh, L. Hall and G. Starkman, SLAC–PUB–4356 (1987).
7. R. V. Wagoner, W. A. Fowler and F. Hoyle, Ab. J. **148** (1967) 493.
8. L. Kowano, D. Schramm, G. Steigman and L. Kowano, Ap. J. **327** (1988) 750.
9. J. Yang, M. S. Turner, G. Steigman, D. Schramm and K. A. Olive, Ap. J. **281** (1984) 493.
10. A. M. Boesgaard and G. Steigman, Ann. Rev. Astr. Ap. **23** (1985) 319.
11. A. Vidal–Madjar, C. Laurent, C. Gry, P. Bruston, R. Ferlet and D. G. York, Astron. Astrophys. **120** (1983) 58.
12. T. Encrenaz and M. Combes, Icarus **52** (1982) 54.
13. J. R. Bond, B. J. Carr and W. D. Arnett, Nature **304** (1983) 514.
14. B. E. J. Pagel, Phil. Trans. R. Soc. A. **307** (1982) 19.
15. R. T. Rood, T. M. Bania and T. L. Wilson, Ap. J. **280** (1984) 629.
16. T. M. Bania et al., as communicated by Boesgaard.
17. D. Kunth in *ESO Workshop on Primordial Helium*, Garching, 335.
18. G. Steigman, J. S. Gallagher III and D. Schramm, Ohio State preprint PRINT–87–0267 (87).

19. F. Spite and M. Spite, Astr. Ap. **115** (1982) 357.

20. J. P. Maurice F. Spite and M. Spite, Astr. Ap. **141** (1984) 56.

21. F. A. Aharonian and V. V. Vardanian, Yerevan Physics Institute preprint 827(54)–85 and M. L. Burns and R. V. E. Lovlace, Ap. J. **262** (1982) 87.

22. R. J. Scherrer and M. S. Turner, Phys. Rev. **D31** (1985) 681.

23. J. Ellis, J. Kim and D. V. Nanopoulos, Phys. Lett. **145B** (1984) 181.

24. L. Brown and D. N. Schramm, preprint FERMILAB–PUB–88/20–A (1988).

Table 1. Hadron shower yields.

ξ_α^K	-10
ξ_d	5
$\xi_{^3\mathrm{H}}$	4
$\xi_{^3\mathrm{He}}$	3
$\xi_{^4\mathrm{He}^*}$	5
$\xi_{^6\mathrm{Li}}$	5×10^{-5}
$\xi_{^7\mathrm{Li}}$	2.5×10^{-6}
$\xi_{^7\mathrm{Be}}$	2.5×10^{-6}
ξ_n	10

FIGURE CAPTIONS

1. The Standard Big Bang predictions of the light element abundances as a function of η for $N_\nu = 3$. a) D, ^{3}He, ^{6}Li and ^{7}Li number densities compared to hydrogen; b) ^{4}He mass fraction.

2. $\mathcal{F}_4(\tau)\exp(-t_4/\tau)$ versus τ.

3. $\mathcal{F}_4(\tau)\exp(-t_7/\tau)$ versus τ.

4. η-independent analytic bounds on $f_X^\circ M_X/f_B$ and $f_X^\circ r_B^*/f_B$. (a) allowed region; (b) forbidden by over-production of ^{7}Li; (c) forbidden by over-destruction of ^{4}He in hadronic showers; (d) forbidden by overphotodissociation of ^{7}Li. Other regions of the parameter space can neither be forbidden nor allowed by analytic arguments.

5. Allowed regions of X parameter space for (a) $\tau = 1\times10^4$ sec; (b) $\tau = 5\times10^4$ sec; (c) $\tau = 1\times10^5$ sec; (d) $\tau = 5\times10^5$ sec, (e) $\tau = 1\times10^6$ sec; (f) $\tau 5\times10^6$ sec; (g) $\tau = 1\times10^7$ sec; The allowed regions are delineated by solid lines, with the source of the limit labeled. Also shown are the bounds obtained by requiring $D+^3\mathrm{He} < 6\times10^4$ (dot-dash lines), $^6\mathrm{Li} < 1\times10^{-10}$ (dotted lines) and $^7\mathrm{Li} < 2\times10^{-10}$ (dashed lines).

6. $\mathcal{G}(\tau)$ and $\mathcal{H}(\tau)$ versus τ.

7. Upper limits on T_{reheat} in the SBBN (solid lines) and DEHS (dotted lines) scenario, over the range of applicable M's, for $N_c = 1, 8, 27, 64$.

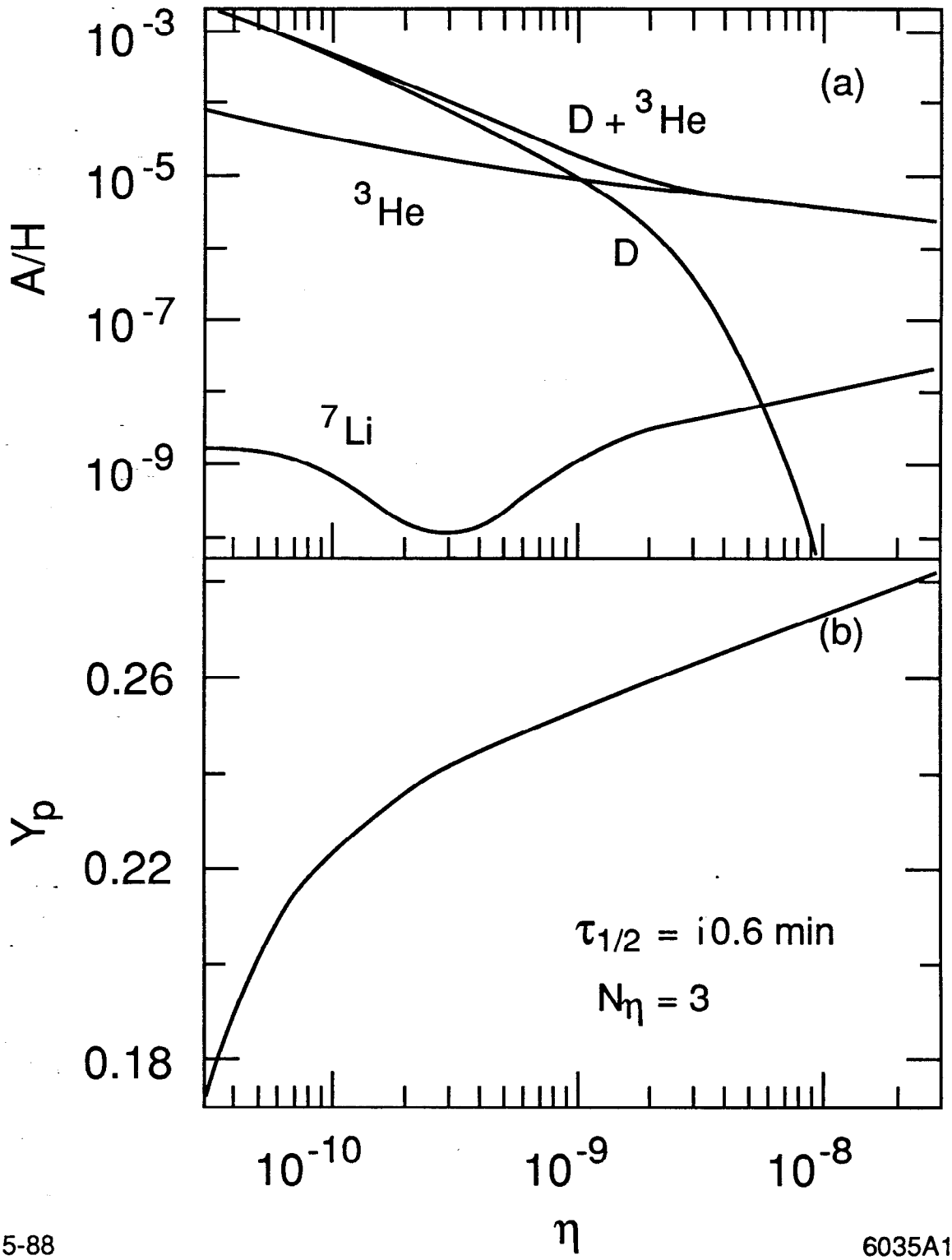
10^-3
10^-5
10^-7
10^-9
A/H
(a)
D + ^3He
^3He
D
^7Li
(b)
0.26
0.22
0.18
Y_p
τ_1/2 = i0.6 min
N_η = 3
10^-10
10^-9
10^-8
η
5-88
6035A1

Fig. 1

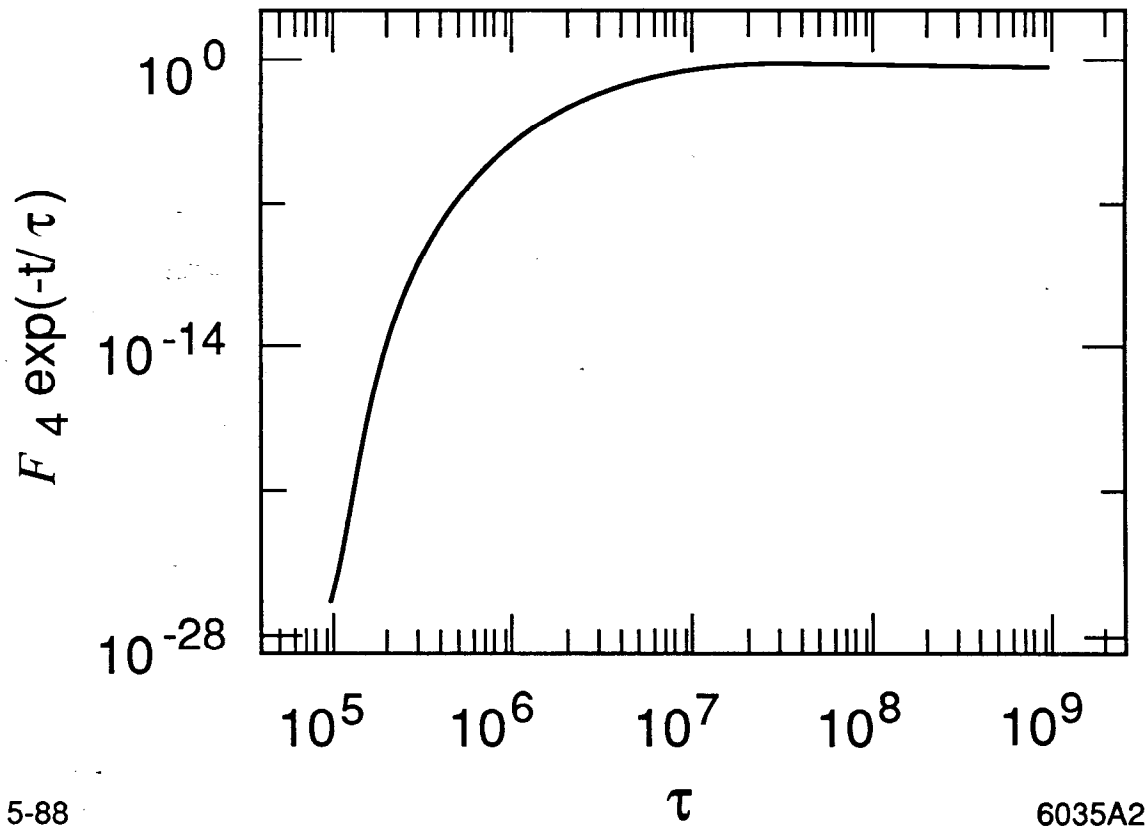

Fig. 2

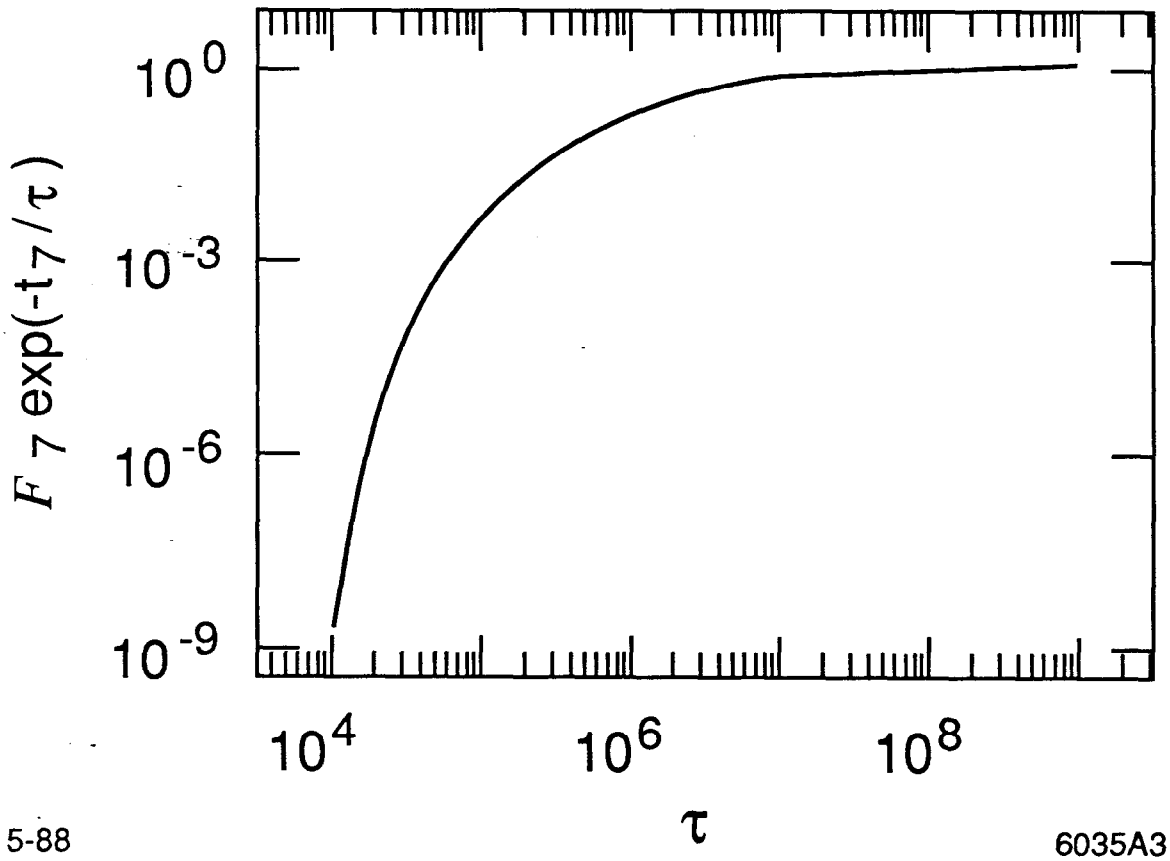

5-88

6035A3

Fig. 3

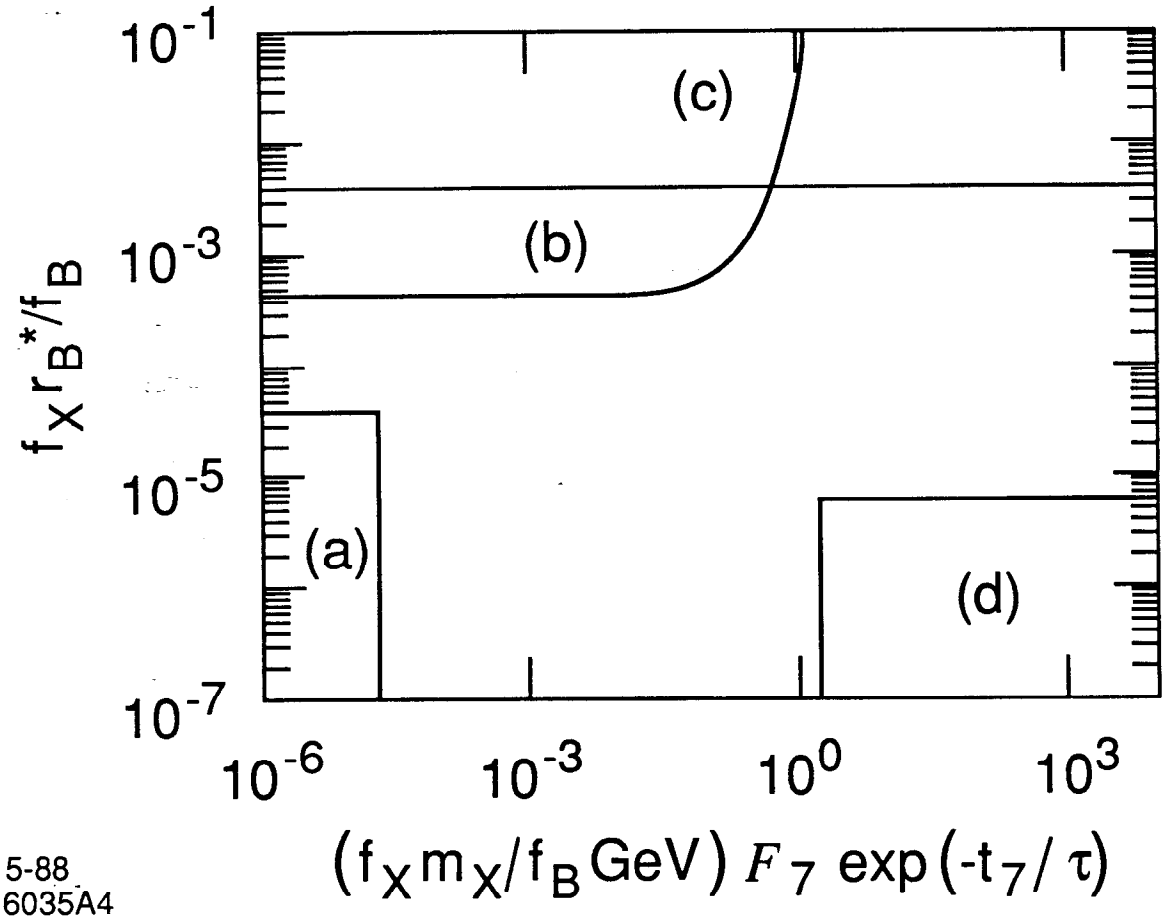

5-88
6035A4

Fig. 4

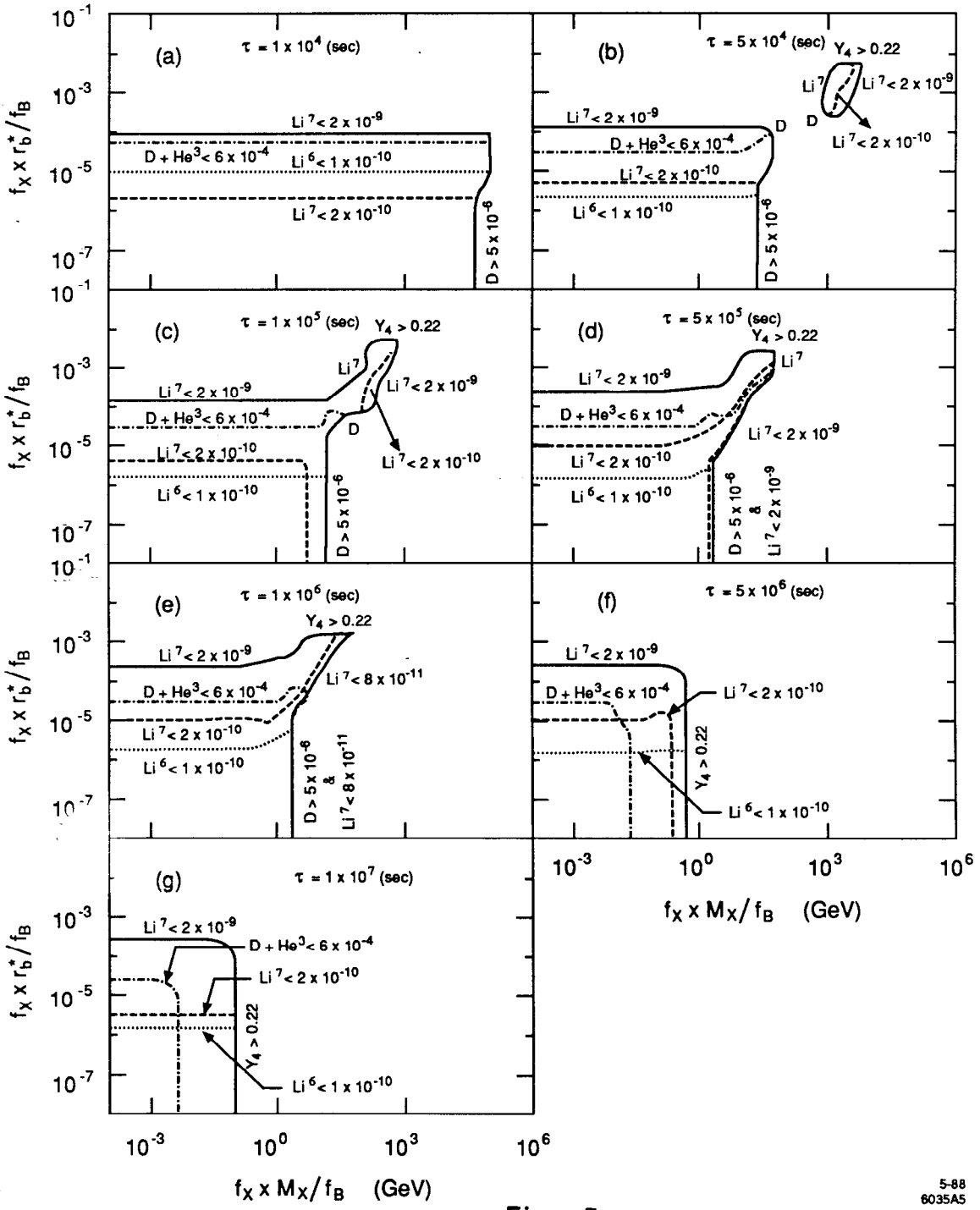

5-88
6035A5

Fig. 5

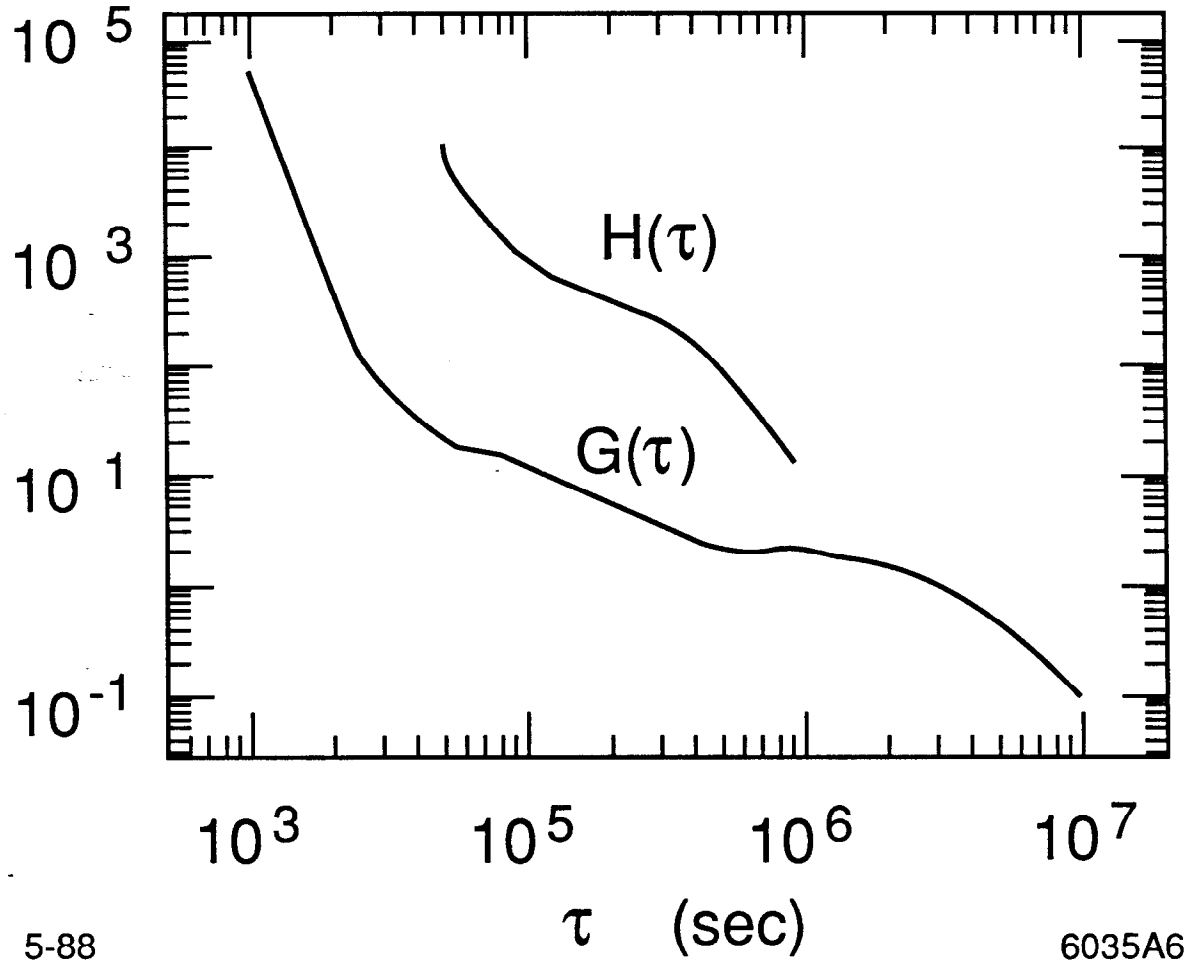

Fig. 6

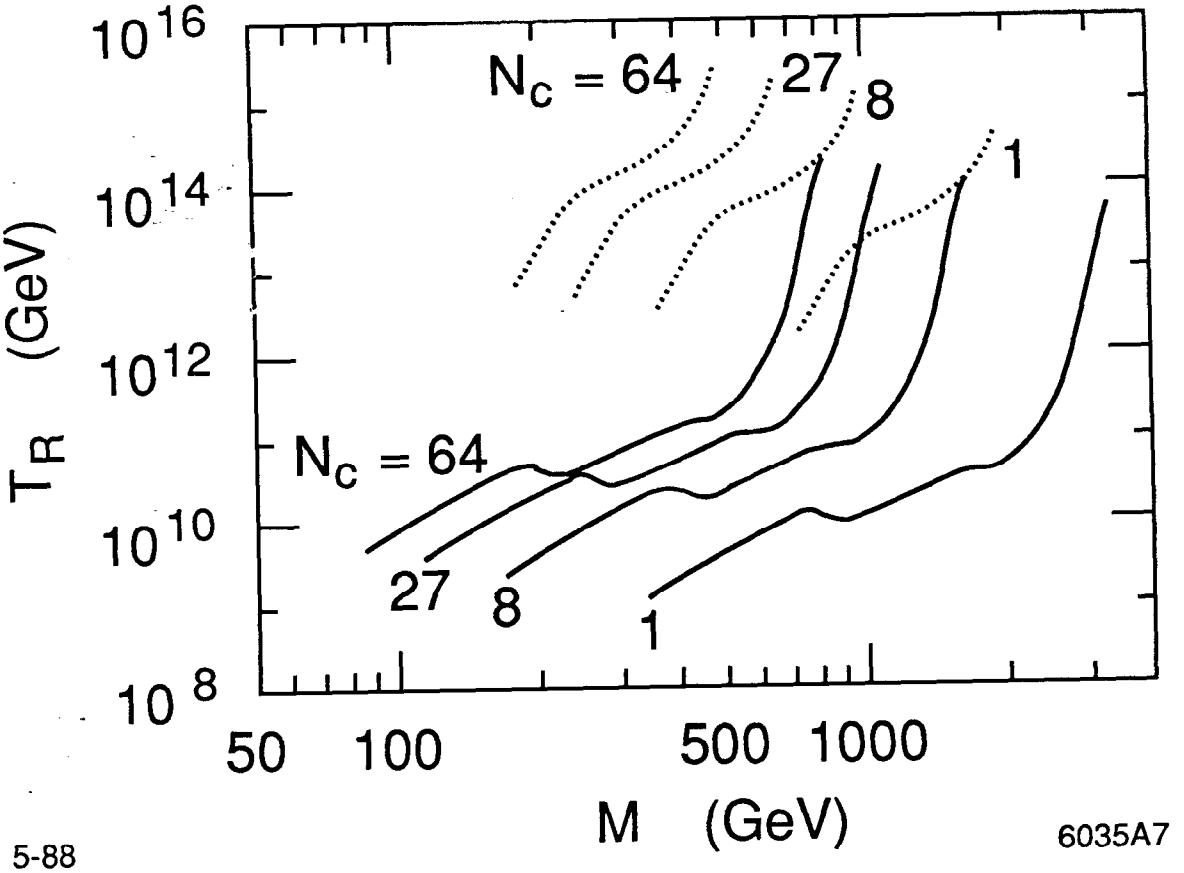
10^{16}
10^{14}
10^{12}
10^{10}
10^{8}
T_R (GeV)
$N_c = 64$
27
8
1
$N_c = 64$
27
8
1
50
100
500
1000
M (GeV)
5-88
6035A7

Fig. 7